Available online at www.sciencedirect.com

SCIENCE DIRECT®

ELSEVIER

International Journal of Mass Spectrometry 252 (2006) 189–196

International Journal of Mass Spectrometry

www.elsevier.com/locate/ijms

Formation of $C_7H_7^+$ ions from ethylbenzene and *o*-xylene ions: Fragmentation versus isomerization☆

Susanne Schulze, Anna Paul, Karl-Michael Weitzel*

Philipps Universität Marburg, Fachbereich Chemie, Hans Meerweinstr., 35032 Marburg, Germany

Received 9 September 2005; received in revised form 21 October 2005; accepted 27 October 2005
Available online 3 April 2006

Abstract

The $C_7H_7^+$ ion, existing in three major isomeric forms (tropylium, benzylium and tolylium), is one of the most fascinating species in organic mass spectrometry. Yet the properties of the three isomers are still under some debate. In a recent experiment we have measured the rate constants for the formation of $C_7H_7^+$ from energy-selected ethylbenzene and *o*-xylene ions [M. Malow, M. Penno, K.M. Weitzel, J. Phys. Chem. A, 107, (2003) 10625]. In the current work we present an extended kinetic analysis taking into account competition of isomerization and fragmentation in both ethylbenzene and *o*-xylene ions. The comparison of the kinetic model with experimental data indicates that isomerization of the precursors to a common intermediate (the methyl-cycloheptatriene ion) prior to fragmentation does not play an important role in the threshold region. Most likely the effective barriers for isomerization of the precursors are significantly higher than the thermochemical onset of fragmentation.

© 2006 Elsevier B.V. All rights reserved.

Keywords: Ion chemistry; Kinetics; Benzylium; Tropylium

1. Introduction

The fragmentation of ethylbenzene ions ($EtBz^{+\bullet}$) has received considerable interest in recent years [1–4]. In part this interest is motivated by the possible products of fragmentation, the benzylium ion (Bz^+) and the tropylium ion ($Trop^+$) which are among the most important species in organic mass spectrometry [5–7]. More recently the fragmentation of $EtBz^{+\bullet}$ ions also served as a model system to test accurate statistical theories with regard to channel switching [8]. One pivotal aspect is the ratio of Bz^+ ions to $Trop^+$ ions formed in the fragmentation. In general the following trend appears to apply. Toluene ion fragmentation leads to a mixture of $Trop^+$ and Bz^+ ions, with the ratio depending on the internal energy of the toluene ions, whereas larger alkyl benzenes (ethyl- [1,9], propyl- [10,11] and butyl-benzene [12]) predominantly lead to Bz^+ ions (>80%).

The conclusion that either Bz^+ or $Trop^+$ ions dominate is often based on secondary reactions, more specifically the observation that Bz^+ ions quantitatively react with toluene [13] and ethylbenzene [9] leaving only the $Trop^+$ ion unchanged. Information on the ratio of Bz^+ to $Trop^+$ being formed has also been derived from the analysis of kinetic energy release (KER) [3,14]. This is possible since formation of Bz^+ is in general believed to proceed by simple bond fission, while formation of $Trop^+$ is associated with a rather tight transition state with a reverse barrier. Ultimately the information of branching ratio $Bz^+/Trop^+$ is also contained in the specific rate constants for product formation, in particular their energy dependence.

In the photodissociation of toluene ions the fraction of benzylium ions increases monotonically with increasing excitation energy in the precursor [9,13]. The actual numbers vary between about 20% Bz^+ close to the threshold and about 70% at higher internal energies. For the ethylbenzene all numbers reported indicate a significantly higher Bz^+ yield. From charge exchange experiments Ausloos concluded that about 80–95% Bz^+ ions are formed from $EtBz^{+\bullet}$ ions—with the ratio $Bz^+/Trop^+$ slightly increasing at low ion internal energies but again decreasing at higher internal energy [9]. In recent work based again on charge exchange experiments Troe et al. [8] concluded that the fraction of Bz^+ increases from about 84% at 2.41 eV ion internal energy to about 95% at 5 eV and decreases again to 84% at 7 eV. A key issue in the question of $Bz^+/Trop^+$ ratio is the isomerization of the precursors. Formation of Bz^+ from $EtBz^{+\bullet}$ proceeds by

---

☆ This paper is dedicated to the memory of Professor Chava Lifshitz.

* Corresponding author. Tel.: +49 6421 282 2360.
E-mail address: weitzel@chemie.uni-marburg.de (K.-M. Weitzel).

1387-3806/$ – see front matter © 2006 Elsevier B.V. All rights reserved.
doi:10.1016/j.ijms.2005.10.016

a simple direct bond fission. Formation of Trop^+ from $\text{EtBz}^{+\bullet}$ requires first isomerization to the methylcycloheptatriene ion ($\text{MeCHT}^{+\bullet}$) with consecutive formation of Trop^+. Such skeleton rearrangement has in fact been observed in mass analyzed ion kinetic energy (MIKE) experiments [15].

The energy dependence of the rate constants for fragmentation of $\text{EtBz}^{+\bullet}$ and o-Xylene$^+$ (o-$\text{Xyl}^{+\bullet}$) ions have been reported by Malow et al. [4] in the range between 1100 and 1200 kJ/mol. Fragmentation of $\text{EtBz}^{+\bullet}$ and o-$\text{Xyl}^{+\bullet}$ predominantly leads to the formation of $C_7H_7{}^+$ ions ($m/z = 91$) by methyl ($\text{Me}^\bullet$) loss, although a small amount of $\text{H}^\bullet$ loss has been observed for o-Xyl. Since the mass spectrometer employed did not distinguish between Bz^+ and Trop^+ the measured rate constants refers to the sum of both product isomers. From the difference between the rate constants measured from $\text{EtBz}^{+\bullet}$ and o-$\text{Xyl}^{+\bullet}$ precursors it was tentatively concluded that isomerization to a common intermediate should not be dominating.

In the current work we further elaborate this hypothesis by putting forward a kinetic model, which for the first time takes into account both isomerization processes and fragmentation processes of $\text{EtBz}^{+\bullet}$ and o-$\text{Xyl}^{+\bullet}$ in a uniform model. By investigating the effect of model $k(E)$ curves on the fragmentation dynamics and comparison with experimental data, we are able to show that fragmentation of $\text{EtBz}^{+\bullet}$ and o-$\text{Xyl}^{+\bullet}$ does not proceed through a common intermediate in the threshold region.

2. The kinetic model

The kinetic model described below is based on a total of seven isomerization and fragmentation steps as depicted in Fig. 1. Each of these steps is associated with a specific rate constant k_i. In order to analyze the relevance of isomerization reactions in the fragmentation of $\text{EtBz}^{+\bullet}$ and o-$\text{Xyl}^{+\bullet}$ ions we have set up a system of coupled rate laws.

$$\frac{d[\text{EtBz}^+]}{dt} = -k_1[\text{EtBz}^+] - k_2[\text{EtBz}^+] + k_3[\text{MeCHT}^+] \qquad (1)$$

$$\begin{aligned}\frac{d[\text{MeCHT}^+]}{dt} &= +k_2[\text{EtBz}^+] - k_3[\text{MeCHT}^+] - k_4[\text{MeCHT}^+] \\ &\quad - k_5[\text{MeCHT}^+] + k_6[o\text{-Xyl}^+] \qquad (2)\end{aligned}$$

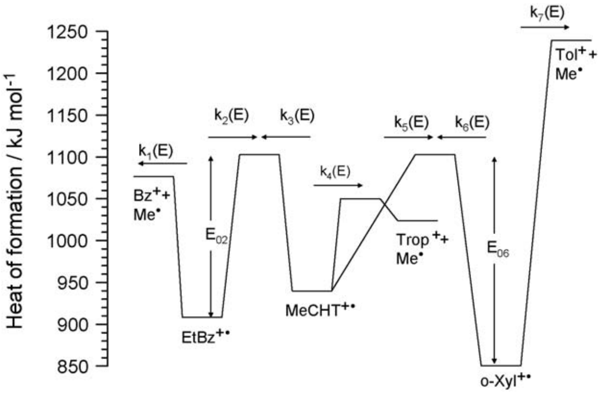

Fig. 1. Energy scheme for the isomerization and fragmentation of ethylbenzene and o-xylene ions.

$$\frac{d[o\text{-Xyl}^+]}{dt} = +k_5[\text{MeCHT}^+] - k_6[o\text{-Xyl}^+] - k_7[o\text{-Xyl}^+] \qquad (3)$$

$$\frac{d[\text{Bz}^+]}{dt} = +k_1[\text{EtBz}^+] \qquad (4)$$

$$\frac{d[\text{Trop}^+]}{dt} = +k_4[\text{MeCHT}^+] \qquad (5)$$

$$\frac{d[\text{Tol}^+]}{dt} = +k_7[o\text{-Xyl}^+] \qquad (6)$$

This system of coupled differential equations involves the concentration of six different species: three parent ions ($\text{EtBz}^{+\bullet}$, $\text{MeCHT}^{+\bullet}$, and o-$\text{Xyl}^{+\bullet}$) and three fragment ions (Bz^+, Trop^+, and Tol^+). The model also involves seven specific rate constants, k_1 to k_7.

Note, that $\text{EtBz}^{+\bullet}$, $\text{MeCHT}^{+\bullet}$ and $\text{Xyl}^{+\bullet}$ are radical cations, whereas the product ions Bz^+, Trop^+ and Tol^+ are closed shell ions. In fact there are four isomers of the $\text{MeCHT}^{+\bullet}$ and three isomers of the $\text{Xyl}^{+\bullet}$ and the Tol^+ ions. The current model does not distinguish between these isomers, but rather summarizes the respective population in one term each.

Using the appropriate boundary conditions as outlined below, we have solved these differential equations numerically employing the Bulirsch-Stoer algorithm provided in MathCad 2001 [16]. This procedure leads to the time dependence of the concentrations of all six species. This time dependence of concentrations can be compared to experimental information regarding fragmentation events in different spectrometer regions of a reflectron. The solution of the rate laws can also be compared to the experimental rate constants reported for the fragmentation of energy selected $\text{EtBz}^{+\bullet}$ and o-$\text{Xyl}^{+\bullet}$ ions [4] and information on the branching ratio available in the literature.

The crucial parameters used in all calculations are the specific rate constants, k_1 to k_7. In principle it would be desirable to calculate these rate constants $k_i(E)$ by unimolecular rate theory. This would, however, require the knowledge of the precise potential depicted in Fig. 1, including the vibrational frequencies of all isomers and transition states involved as well as rotational constants and threshold energies. Some of this information is now emerging for the dissociation of $\text{EtBz}^{+\bullet}$ [2,8]. For the other relevant processes reliable information is currently not available. Attempts to calculate $k(E)$ curves by standard RRKM rate theory were not successful. In particular for the Trop^+ channel adjustment of several parameters was required.

In the current context it is not primarily the absolute value of the rate constant, which is important, but rather the relative magnitude of the $k_i(E)$, which determines e.g. the branching ratio. In this situation we decided to employ simple, empirical models for representing the $k_i(E)$ curves. The number of parameters used in these empirical models is certainly not larger than that we would have to adjust in using more sophisticated rate theories.

Table 1
Threshold energies $E_{o,i}$ in kJ/mol

	$E_{0,1}$	$E_{0,2}$	$E_{0,3}$	$E_{0,4}$	$E_{0,5}$	$E_{0,6}$
Relative to ion ground state	168	193	160	110	160	240
Absolute $\Delta H_f(0K)$	1075	1100	1100	1050	1100	1100

Numbers are given relative to the respective ion ground state and on an absolute scale. Note that the values $E_{0,2}$ and $E_{0,3}$ are connected via the energy difference between $EtBz^{+\bullet}$ and $MeCHT^{+\bullet}$ of 33 kJ/mol. $E_{0,5}$ and $E_{0,6}$ are connected via the energy difference between $MeCHT^{+\bullet}$ and o-$Xyl^{+\bullet}$ of 80 kJ/mol. One set of calculations is performed starting from pure $EtBz^{+\bullet}$, another from pure o-$Xyl^{+\bullet}$ precursors. Ultimately the parameters are varied in nested loops in order to minimize the deviation between experiment and model; for comparison see Fig. 1.

3. Results and discussion

3.1. RRK-type k(E) curves

In the first part of the analysis all specific rate constants have been calculated within the RRK model [17,18]

$$k_i(E) = A\left(\frac{E - E_{o,i}}{E}\right)^s \tag{7}$$

where A, $E_{o,i}$ and s are empirical parameters. Being aware of the simplification, the advantage of the model certainly is in the physical interpretation of the threshold energies $E_{o,i}$. Here our primary interest is focused on the barriers for isomerization, $E_{0,2}$ and $E_{0,5}$, in particular to find out if these barriers occur below the onset of fragmentation or above. In the former case isomerization of the reactants prior to fragmentation should play a central role, in the latter case not.

The differential rate laws described above were solved numerically systematically varying the threshold energies $E_{0,2}$, $E_{0,5}$ and the ion internal energy. For simplicity the parameters A and s were set to $9.74 \times 10^9\ s^{-1}$ and 7.47, respectively for all k_i [4]. The rate constant k_7 is set to zero, since formation of Tol^+ is not expected to be relevant in the energy range of interest [19]. For the same reason a possible isomerization of Bz^+ to $Trop^+$ has not been taken into account. The limitations introduced by this approximation will be discussed at a later point. The threshold energy $E_{0,1}$ is well known to be 168 kJ/mol [4,20], $E_{0,4}$ is set to 110 kJ/mol from a combination of the heats of formation of $EtBz^{+\bullet}$, $MeCHT^{+\bullet}$ and the assumption of a reverse barrier for $Trop^+$ formation of 30 kJ/mol [3,21]. All threshold energies are given in Table 1. These numbers are also the basis of Fig. 1. The numbers given for E_{02} and E_{05} are those for which the rms of deviation between experiment and model becomes minimum (see below). The specific rate constant curves $k_i(E)$ are illustrated in Fig. 2.

The primary result of solving the rate laws is the time dependence of the relevant concentrations. Fig. 3 shows a typical time dependence of the concentration of $EtBz^{+\bullet}$, Bz^+ and $Trop^+$ at an absolute energy of 1150 kJ/mol. The decay of the parent ion $EtBz^{+\bullet}$ is mono exponential, as is the increase in fragments Bz^+ and $Trop^+$. The effective time constant obtained from fitting an exponential law to these numerical data is $k = 1.6 \times 10^6\ s^{-1}$. The experimental rate constant observed at this energy is $1.3 \times 10^6\ s^{-1}$ [4]. We will come back to this point below. While the PEPICO experiment is not sensitive to the structure of the fragment ion—it measures the sum of $Bz^+ + Trop^+$ yields—the current numerical analysis does distinguish Bz^+ and $Trop^+$. At the energy used in Fig. 3 the ratio of Bz^+:$Trop^+$ is 96.5:3.5. Thus, fragmentation of $EtBz^{+\bullet}$ at 1150 kJ/mol is predicted to predominantly lead to Bz^+. With increasing internal energy in the $EtBz^{+\bullet}$ ion isomerization to the $MeCHT^{+\bullet}$ becomes accessible. Consequently, the yield of $Trop^+$ ions increases with the ion internal energy. Note that the energy range covered in the PEPICO experiment by Malow et al. [4] spans from about 92000–100000 cm^{-1} (1100–1200 kJ/mol).

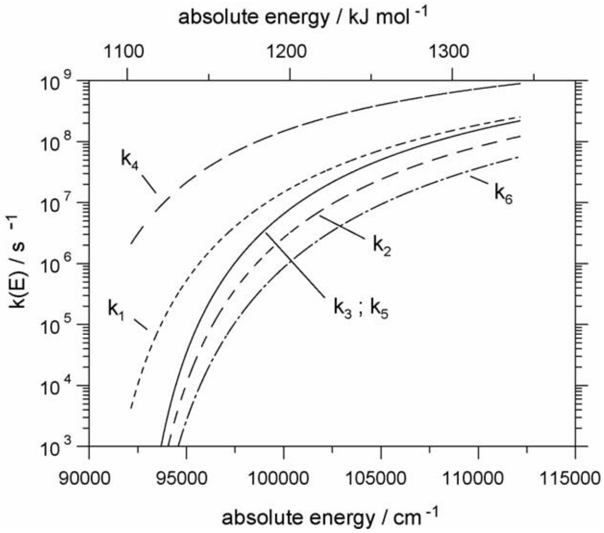

Fig. 2. Model rate constant curves for the six isomerization and fragmentation processes discussed in the text.

While the results presented above apply to an experiment starting from pure $EtBz^{+\bullet}$, the following analysis applies to an experiment starting from pure o-$Xyl^{+\bullet}$. Isomerization of o-$Xyl^{+\bullet}$ first leads to intermediate $MeCHT^{+\bullet}$, which then dissociates to form $Trop^+$ or further isomerizes to $EtBz^{+\bullet}$ and ultimately leads to Bz^+. Thus, the analysis of o-$Xyl^{+\bullet}$

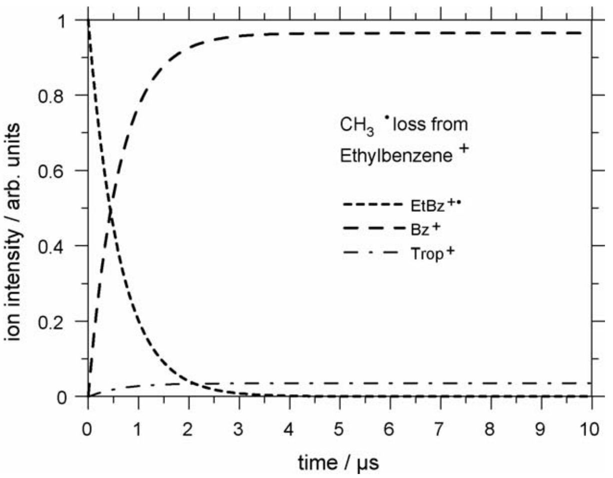

Fig. 3. Calculated time dependence of concentrations, $EtBz^{+\bullet}$, Bz^+, and $Trop^+$ for $Me^\bullet$ loss from $EtBz^{+\bullet}$.

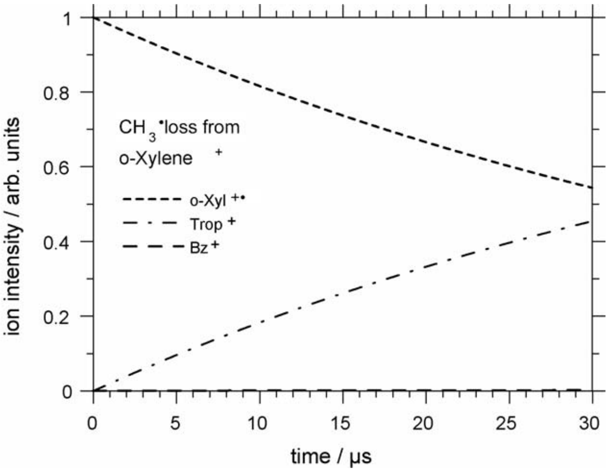

Fig. 4. Calculated time dependence of concentrations, *o*-Xyl$^{+•}$, Bz$^+$, and Trop$^+$ for Me$^•$ loss from *o*-Xyl$^{+•}$.

fragmentation is sensitive to both barriers $E_{0,6}$ and $E_{0,2}$. It turned out that barrier $E_{0,6}$ basically determines the absolute rate constant for *o*-Xyl$^{+•}$ fragmentation. Barrier $E_{0,2}$ determines the ratio of Trop$^+$ to Bz$^+$ yield. This in turn directly affects the time evolution of product formation. Here again all experimental evidence suggests that the formation of $C_7H_7^+$ follows a mono exponential rate law [4]. Using a barrier $E_{0,2}$ significantly smaller than 193 kJ/mol would lead to a pronounced deviation from mono exponential formation of $C_7H_7^+$. It would also lead to an energy dependence of the effective rate constant not compatible with the experimental information.

For illustration Fig. 4 shows the time evolution of product formation from *o*-Xyl$^{+•}$ at an absolute energy of 1150 kJ/mol. Note that no significant amount of Bz$^+$ is observed under these conditions. *o*-Xyl$^{+•}$ appears to exclusively fragment to form Trop$^+$. The effective rate constant predicted for formation of $C_7H_7^+$ is $2 \times 10^4\ s^{-1}$. The experimental value is $3.3 \times 10^4\ s^{-1}$ [4].

As indicated above the two barrier heights for isomerization, (i) *o*-Xyl$^{+•}$ $\leftrightarrows$ MeCHT$^{+•}$, $E_{0,6}$ ($E_{0,5}$) and (ii) EtBz$^{+•}$ $\leftrightarrows$ MeCHT$^{+•}$, $E_{0,2}$ ($E_{0,3}$) were varied until best agreement between the modelled rate constant for formation of $C_7H_7^+$ (i.e. Trop$^+$ + Bz$^+$) and the experimental information [4] was obtained. The variation of both barriers was cut off at an upper limit of the energy of 1100 kJ/mol. At that energy fragmentation of *o*-Xyl$^{+•}$ is observed experimentally. Since the fragmentation of *o*-Xyl$^{+•}$ requires isomerization, the barrier for the latter can not be higher than 1100 kJ/mol. This argument does not strictly apply to the EtBz$^{+•}$. As it turns out the optimized parameters are $E_{0,2} = 193$ kJ/mol relative to the energy of EtBz$^{+•}$ (absolute position of barrier: 1100 kJ/mol) and $E_{0,6} = 240$ kJ/mol relative to the energy of *o*-Xyl$^+$ (absolute energy of barrier: 1100 kJ/mol), which is basically the highest energy considered. The sensitivity of the analysis will be discussed below. Fig. 5 shows the effective rate constants for Me$^•$ loss from EtBz$^{+•}$, $k_{\rm EtBz}$, and *o*-Xyl$^{+•}$, $k_{o\text{-Xyl}}$, obtained in the current analysis together with the measured data [4]. Evidently the agreement is nice for EtBz$^{+•}$. For the *o*-Xyl$^{+•}$ also reasonable agreement is observed at intermediate and high energy. At low energy (threshold region) differences emerge, which will be discussed below.

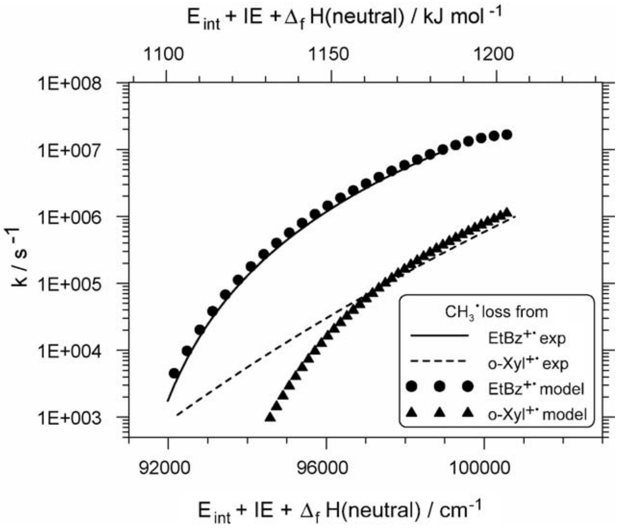

Fig. 5. Comparison of effective rate constants for Me$^•$ loss from EtBz$^{+•}$ and *o*-Xyl$^{+•}$. Symbols: this work; lines: experimental data from Malow et al. [4].

The analysis presented above has led to the time dependence of Bz$^+$ and Trop$^+$ ion yields which can be compared to other information available in the literature. Assuming that both barriers of isomerization $E_{0,2}$ (EtBz$^{+•}$ $\leftrightarrows$ MeCHT$^{+•}$) and $E_{0,6}$ (*o*-Xyl$^{+•}$ $\leftrightarrows$ MeCHT$^{+•}$) occur significantly below the absolute threshold for formation of Bz$^+$ inevitably leads to a situation where the effective rate constants for Me$^•$ loss from EtBz$^{+•}$ and *o*-Xyl$^{+•}$ become comparable within a factor of 2. This is clearly in disagreement with the experimental data from Malow et al. [4], which show up to a factor of 50 difference at intermediate energy (1150 kJ/mol). Increasing the threshold $E_{0,6}$ would concomitantly decrease the rate constant for Me$^•$ loss from *o*-Xyl$^{+•}$, thus leading to a more favourable ratio of $k_{\rm EtBz}$ to $k_{o\text{-xyl}}$. However, a low barrier $E_{0,2}$ would still cause isomerization EtBz$^{+•}$ $\leftrightarrows$ MeCHT$^{+•}$. In this case EtBz$^{+•}$ would in part isomerize all the way to *o*-Xyl$^{+•}$, which would function as an effective sink. From this sink population would come back with some time delay causing a pronounced deviation from mono exponential decay of EtBz$^{+•}$ incompatible with the experiment. This non-exponential decay only disappears at barriers $E_{0,6}$ in the region of 240 kJ. However, then *o*-Xyl$^{+•}$ does not represent a sink for Me$^•$ loss from EtBz$^{+•}$ and the ratio of $k_{\rm EtBz}$ to $k_{o\text{-xyl}}$ becomes too large. A combination of intermediate barrier height $E_{0,2}$ (169 kJ/mol) with low and intermediate barrier height $E_{0,6}$ yields ratios $k_{\rm EtBz^+}$ to $k_{o\text{-xyl}}$ which are too small.

The combination of intermediate barrier $E_{0,2}$ (169 kJ/mol) and high barrier $E_{0,6}$ can not be ruled out based on our current analysis; however, it does not lead to the best agreement between model and experiment. Combination of high barrier $E_{0,2}$ (193 kJ/mol) and low and intermediate barrier $E_{0,5}$ again causes a too small ratio $k_{\rm EtBz}$ to $k_{o\text{-xyl}}$. Finally the combination of high barriers $E_{0,2}$ (193 kJ/mol) and $E_{0,6}$ (240 kJ/mol) leads to the best agreement between experimental data and the current model. We intentionally discussed the implications of this kinetic analysis in terms of a simple picture of threshold energies.

The advantage obviously is that it serves the purpose of illustration. We stress that the analysis itself is solely based on the $k(E)$ curves entering into the rate laws. In fact we could use any other kinetic model to generate the $k(E)$ curves. The important point is, that among all the RRK-type $k(E)$ curves investigated in this work the ones shown in Fig. 2 lead to the best agreement between the kinetic model and the experiment. The results of this analysis imply that isomerization of $\mathrm{EtBz}^{+\bullet}$ and o-$\mathrm{Xyl}^{+\bullet}$ to a common intermediate prior to fragmentation does not play an important role.

There are two minor points, where the $k(E)$ curves discussed above may turn out to deviate from the true ones. First, the current approach predicts, that the fraction of Trop^+ yield from $\mathrm{EtBz}^{+\bullet}$ should increase from 0 to 15% in going from 1100 to 1200 kJ/mol. At higher energy it would further increase. All experimental evidence currently available suggests that the fraction of Trop^+ runs through a maximum of 15% at about 1150 kJ/mol [8,9]. This would be reproduced by the current kinetic model if the logarithmic plot of $k_2(E)$ for isomerization $\mathrm{EtBz}^{+\bullet} \leftrightarrows \mathrm{MeCHT}^{+\bullet}$ is more curved than that for Bz^+ formation, $k_1(E)$. This would disfavour isomerization even more and would not alter any of the conclusions presented above.

The other point relates to the deviation between the modelled effective rate constant for $\mathrm{Me}^\bullet$ loss from o-$\mathrm{Xyl}^{+\bullet}$ and the experimental one. This discrepancy at low energy is due to the fact that the curvature of the $\log k_6(E)$ versus E plot employed is too large compared to the experiment. Already Malow et al. [4] noticed that the experimental rate constant for Me loss from o-$\mathrm{Xyl}^{+\bullet}$ is not best described by a RRK approach. Yet, for a first analysis we felt it was appropriate to stay within one $k(E)$ model. Below we will discuss improved model calculations. As mentioned above, in any case more accurate $k(E)$ curves can easily be put into the current kinetic model as they become available.

3.2. Modified k(E) curves

In the following we have further modified the model $k_i(E)$ curves for the processes $i = 1, 2$ and 6. In particular for $k_2(E)$ and $k_6(E)$ we needed a different empirical $k(E)$ expression allowing for a more flexible representation of curvatures in a logarithmic $k(E)$ plot. Such an empirical formula as given in (8) has been suggested by Troe [22] and successfully applied to $\mathrm{EtBz}^{+\bullet}$ [2] and o-$\mathrm{Xyl}^{+\bullet}$ [4] dynamics.

$$k_i(E) = A_i\left(\frac{E - E_{o,i}}{p}\right)^{s_i} \tag{8}$$

In principle Eq. (8) could be written in a three parameter form. The reason for using Eq. (8) is connected to the comparison to high energy data. Table 2 lists the optimized parameters for the rate constant curves $k_i(E)$, with $i = 1, 2, 4$ and 6.

Here k_1 and k_2 were adjusted in order to match the experimental $\mathrm{Trop}^+/\mathrm{Bz}^+$ ion yields. For an illustration Fig. 6 shows the experimental fragment ion yields from $\mathrm{EtBz}^{+\bullet}$ at various internal energies [8,9] together with our improved model. Keeping in mind that the experimental information might be subject to secondary processes at higher internal energies the agreement between experiment and model appears reasonable. Note, that the absolute scaling factors for k_1 and k_2 were adjusted in order to match the experimental rate constants for $\mathrm{EtBz}^{+\bullet}$ decay. As it turns out four $k_i(E)$ curves (k_1, k_2, k_4, k_6) are truly dominating the dynamics of both $\mathrm{EtBz}^{+\bullet}$ and o-$\mathrm{Xyl}^{+\bullet}$ fragmentation (c.f. Table 2).

Table 2
Parameters employed in the modified empirical rate constants $k_i(E)$

	A_i (s^{-1})	$E_{o,i}$ (kJ/mol)	s_i	p_i (kJ/mol)	Model equation
k_1	7.09×10^9	168	7.47	n.a.	(7)
k_2	9.67×10^{12}	193	2.84	2.605×10^4	(8)
k_4	9.74×10^9	110	7.47	n.a.	(7)
k_6	3.93×10^8	13.5	18.45	459.6	(8)

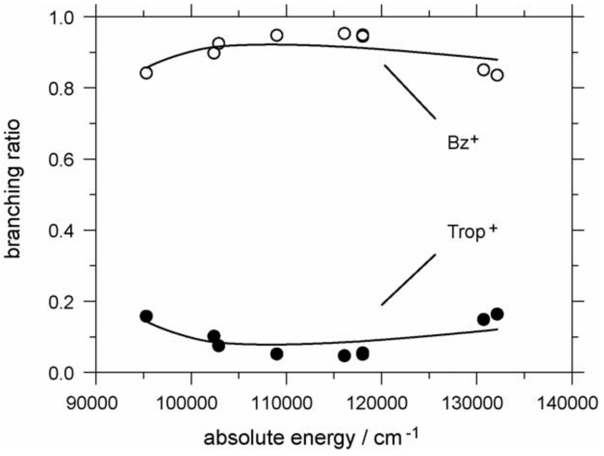

Fig. 6. Comparison of experimental and modelled Trop^+ and Bz^+ ion yields: exp. data from [6]; modelled data: this work.

The resulting $k(E)$ curves are illustrated in Fig. 7. Over the entire energy range covered $k_4(E)$, i.e. the fragmentation of $\mathrm{MeCHT}^{+\bullet}$ is the fastest process. This implies that basically all population intermediately arriving in the $\mathrm{MeCHT}^{+\bullet}$ conformation is directly transferred to Trop^+. Reisomerization of $\mathrm{MeCHT}^{+\bullet}$ to either $\mathrm{EtBz}^{+\bullet}$ (k_3) or o-$\mathrm{Xyl}^{+\bullet}$ (k_5) appears to be negligible. Over most of the energy range shown, the slope of

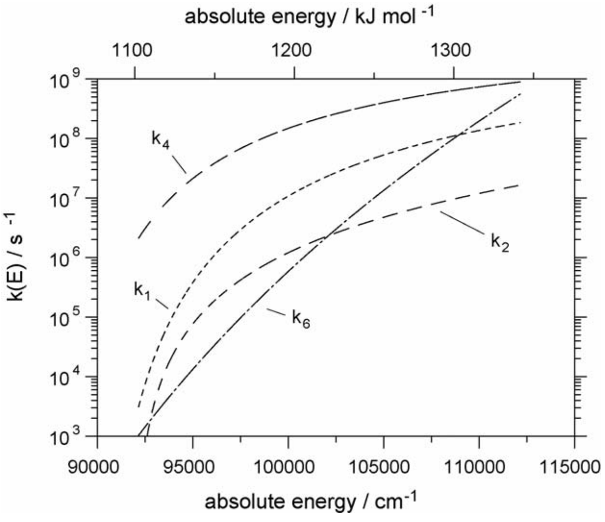

Fig. 7. Improved model rate constant curves. For further details see text.

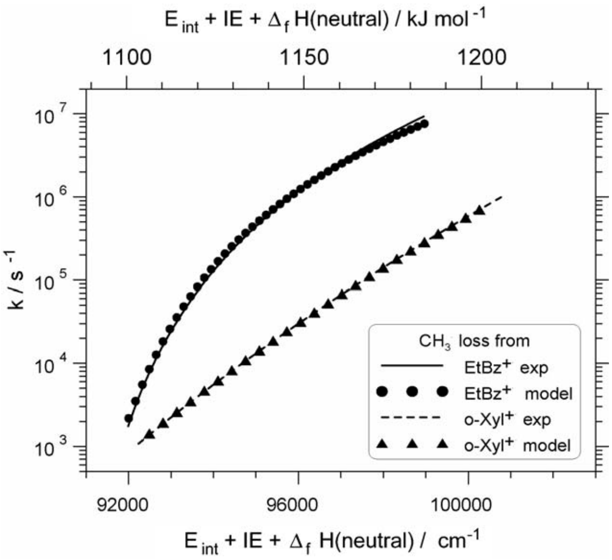

Fig. 8. Comparison of effective rate constants for Me$^\bullet$ loss from EtBz$^{+\bullet}$ and *o*-Xyl$^{+\bullet}$. Symbols: this work (improved model); lines: experimental data from Malow et al. [4].

the $k_2(E)$ is smaller than that of $k_1(E)$. At even higher energies the situation is reversed. This directly reflects the fact that the relative yield of Bz$^+$ runs through a maximum and that of Trop$^+$ through a minimum at intermediate energy (c.f. Fig. 6). The plot of $k_6(E)$ has by far the smallest curvature. As we will show below this leads to improved agreement with experimental rate constants for Me loss from *o*-Xyl$^{+\bullet}$. In the energy range of the experimental $k(E)$ data there is strong evidence that k_3 and k_5 are at least one order of magnitude smaller than k_4, and thus negligible.

Ultimately we have recalculated the effective rate constant for Me$^\bullet$ loss from EtBz$^{+\bullet}$ and *o*-Xyl$^{+\bullet}$ based on the rate constants shown in Fig. 7. The result is shown in Fig. 8 in comparison with the experimental data from Malow et al. [4]. Evidently the agreement is now very good for both molecules over the entire energy range. Thus, we are confident that the kinetic model and the rate constants presented provide an appropriate picture of the energetics and dynamics of EtBz$^{+\bullet}$ and *o*-Xyl$^{+\bullet}$ fragmentation.

4. Summary and discussion

In the current work we have for the first time proposed a uniform kinetic model taking into account specific isomerization and fragmentation steps of both EtBz$^{+\bullet}$ and *o*-Xyl$^{+\bullet}$ ions. The analysis employed empirical model rate constants leading to an improved understanding of the mechanism. The results indicate that fragmentation of EtBz$^{+\bullet}$ predominantly leads to Bz$^+$ ions. The effective rate constant for Me$^\bullet$ loss from EtBz$^{+\bullet}$ turns out to be equal to the sum of specific rate constants k_1 (C–C bond fission in EtBz$^{+\bullet}$) + k_2 (isomerization EtBz$^{+\bullet}$ $\leftrightarrows$ MeCHT$^{+\bullet}$). The modelled rate constants agree nicely with the experimental data from Malow et al. [4]. The relative yield of Trop$^+$ and Bz$^+$ ions from EtBz$^{+\bullet}$ also agrees with experimental information [8,9]. In the threshold region around 92000 cm^{-1} the modelled k_2 curve exhibits a rather large slope. If the barrier for isomerization of EtBz$^{+\bullet}$ to MeCHT$^{+\bullet}$ was in fact lower than assumed, the amount of Trop$^+$ would concomitantly increase. However, the kinetic conclusions of this work would remain unaltered. Currently the smallest absolute energy for which experimental information on the Bz$^+$/Trop$^+$ ratio is available is about 95000 cm^{-1} [8,9]. It would be very interesting to see experimental data at lower energy, perhaps by using a chemical ionizer of lower ionization energy.

The effective rate constant for Me$^\bullet$ loss from *o*-Xyl$^{+\bullet}$ is equal to k_6 (isomerization *o*-Xyl$^{+\bullet}$ $\leftrightarrows$ MeCHT$^{+\bullet}$). Again the modelled data agree nicely with experimental data from Malow et al. [4]. The model suggests that only Trop$^+$ is formed at the threshold of *o*-Xyl$^{+\bullet}$ fragmentation. No accurate experimental data on this specific precursor is currently available to our knowledge. We note, however, that Viggiano and coworkers reported that about 70–80% of the $C_7H_7{}^+$ ions formed from *m*-Xyl$^{+\bullet}$ have the Bz$^+$ structure [1]. The slope of the k_6 curve appears unusual for an isomerization process. Here, we can not exclude the possibility that the effective rate constant for isomerization of *o*-Xyl$^{+\bullet}$ is actually a result of a composite process involving more than one transition state. We hope that this work stimulates future experimental studies in particular of the fragmentation and isomerization of *o*-Xyl$^{+\bullet}$.

The question whether isomeric ions formed by electron impact ionization retain specific properties has been investigated extensively by Dunbar [23,24]. The photodissociation spectra of EtBz$^{+\bullet}$, and *o*-, *m*- and *p*-Xyl$^{+\bullet}$ appear to be distinguishable in principle. This is most likely due to the fact that isomerization was slower than thermalization on the time scale of the experiment. Since photodissociation spectra are in general recorded at low pressure ($\approx 10^{-7}$ mbar) and thus thermalization must be rather slow itself, this further supports the conclusion of the present work.

Information regarding the competition between isomerization and fragmentation of $C_8H_{10}{}^{+\bullet}$ ions is also available from MIKES experiments. Williams et al. have investigated the kinetic energy release (KER) in the metastable decay of EtBz$^{+\bullet}$, 7-MeCHT$^{+\bullet}$, and the three isomers *o*-Xyl$^{+\bullet}$, *m*-Xyl$^{+\bullet}$ and *p*-Xyl$^{+\bullet}$ [25]. For both EtBz$^{+\bullet}$ and MeCHT$^{+\bullet}$ the average KER measured for fragmentation in the second field free region (FFR) of a multi-sector mass spectrometer was reported as 11.6 kJ/mol. The KER for fragmentation of all three xylene isomers was reported to be about 14.7 kJ/mol. Similar results were observed by Kim et al. [3]. In addition Kim et al. reported the KER distributions (KERD) for the metastable decay of $C_8H_{10}{}^{+\bullet}$ ions. For all precursors a bimodal KERD was derived indicating the contribution of two mechanistic reaction channels. The channel associated with a thermal KERD was attributed to the formation of Bz$^+$, the channel with large non-thermal KERD to the formation of Trop$^+$. From their data the authors concluded that isomerization between EtBz$^{+\bullet}$ and MeCHT$^{+\bullet}$ is fast, while isomerization of Xyl$^{+\bullet}$ to the MeCHT$^{+\bullet}$ is slow. The latter agrees with the conclusion of this work, the former not. In principle it would be desirable to even derive the ratio of Bz$^+$ to Trop$^+$ yields from such analysis as e.g. described for toluene [14]. However, we are not aware of such an analysis for the $C_8H_{10}{}^{+\bullet}$ system.

One problem might be associated with the internal energy distribution of the precursor ions, which is in general difficult to obtain in a MIKES experiment. Note, that the internal energy of $EtBz^{+\bullet}$ and o-$Xyl^{+\bullet}$ ions in the $k(E)$ measurement of [4] is precisely known, due to the energy selection in the photoelectron photoion coincidence technique (PEPICO) [26]. The internal energy of parent ions is also reasonably well established in charge exchange experiments provided that the assumption of resonance energy transfer is applicable [27,28]. In general the analysis of MIKES experiments is based on the assumption that fragmentation in the second FFR originates from parent ions with very low internal energy. However, one should bear in mind that MIKES is based on life-time selection of parent ions. Therefore, fragmentation events on the μs time scale could also originate from population of the parent ions temporarily trapped in any local minimum of the potential energy surface before recovering. For a quantitative interpretation it would be helpful to know the relative intensity of fragment yields in the second field free region compared to that in the other spectrometer regions. This information is usually difficult to obtain. Kim et al. also reported the KER in the photodissociation of $EtBz^{+\bullet}$ and $Xyl^{+\bullet}$ ions [3]. Here a mono modal KERD was observed, indicating that the Bz^+ channel dominates. The internal energy in these PD experiments was estimated to be on the order of 4 eV corresponding to an absolute energy of 1295 kJ/mol. This in turn corresponds approximately to that energy where in fact a minimum in the relative $Trop^+$ yield was observed [8,9]. Further information on the dynamics of $C_8H_{10}^{+\bullet}$ fragmentation comes from MIKES experiments with labelled compounds. Extensive studies of ^{13}C labelled [15] and D labelled [29] $C_8H_{10}^{+\bullet}$ ions have been reported by Grotemeyer and Grützmacher. In general the fragment ion yields observed from decay in the ion source and the first FFR exhibit little scrambling, while decay in the second FFR is associated with rather strong scrambling. For example in $EtBz^{+\bullet}$ loss of terminal $^{13}CH_3^{\bullet}$ dominates in all spectrometer regions, however, the amount of $^{12}CH_3^{\bullet}$ lost increases from 10.5% in the ion source to 27% in the second FFR. Similarly for $^{13}CH_3$ labelled p-xylene loss of $^{13}CH_3^{\bullet}$ amounts to 50.1% in the ion source, 34% in the first FFR but only 13.2% in the second FFR. This seems to suggest that parent ions undergo extensive scrambling, i.e. isomerization, at low internal energy, but show site specific fragmentation with little isomerization at high internal energy. However, these results from the second FFR are not compatible with the PEPICO experiments from [4]. At this point we can only speculate that if isomerization takes place, revisiting the dissociative part of the potential energy surface may occur at a later time leading to the observed fragmentation in the second FFR. The possibility of kinetic trapping has in fact already been discussed by Grotemeyer et al. [15]. The correlation of second FFR decay with parent ions of low internal energy remains questionable. At 11.7 eV excitation energy the PEPICO spectra of ETBz showed about 90% decay in the ion source [4]. The effective rate constant was on the order of $3 \times 10^6\,s^{-1}$. For o-Xyl at 11.7 eV 30% of the fragmentation occurs in the ion source, 50% in the first field free drift region [4]. Here the effective rate constant was on the order of $7 \times 10^4\,s^{-1}$. Thus, the PEPICO data of [4] should not be compared to decay in the second FFR but to decay in the ion source and in the first FFR of the MIKES experiments performed at 12 eV electron impact energy [15]. Here we conclude that PEPICO data, MIKES data and the current analysis are all compatible.

From this the following picture emerges. Fragmentation of o-$Xyl^{+\bullet}$ ions occurs by slow rate determining isomerization to the $MeCHT^{+\bullet}$ followed by fast fragmentation to $Trop^+$. Isomerization of the intermediate $MeCHT^{+\bullet}$ to the $EtBz^{+\bullet}$ followed by fragmentation into the Bz^+ channel can not effectively compete against the $Trop^+$ channel. Fragmentation of $EtBz^{+\bullet}$ predominantly leads to the formation of Bz^+ ions. Isomerization of $EtBz^{+\bullet}$ to the $MeCHT^{+\bullet}$ is expected to be of minor importance. However, it can not be ruled out rigorously. If $MeCHT^{+\bullet}$ is intermediately formed from $EtBz^{+\bullet}$ it most likely fragments into the $Trop^+$ channel in a fast process. Further isomerization to the $Xyl^{+\bullet}$ region of the potential energy surface does not seem likely. Of course these conclusions do only apply at energies where isomerization of the products (Bz^+ and $Trop^+$) does not occur. In the energy range below 1200 kJ/mol this can be safely excluded.

As an outlook we note that there are several possible experiments which could shed further light onto the current problem. The first is the measurement of the ratio of Bz^+ to $Trop^+$ yields for o-Xyl and for MeCHT, analogous to the EtBz work [8]. This would require additional information on the reaction between Bz^+ and $Trop^+$ with the corresponding precursor. The second rewarding experiment would be the measurement of the rate constant $k(E)$ for $Me^{\bullet}$ loss from energy-selected $MeCHT^{+\bullet}$ ions and m-Xyl and p-Xyl. Unfortunately we are currently not in the position to provide the latter information. In addition, high level ab initio calculations on the reaction path leading from the xylene ions to the $C_7H_7^+$ fragments would be very helpful.

References

[1] S.T. Arnold, I. Dotan, S. Williams, A.A. Viggiano, R.A. Morris, J. Phys. Chem. A 104 (2000) 928.

[2] J. Troe, A.A. Viggiano, S. Williams, J. Phys. Chem. A 108 (2004) 1574.

[3] Y.H. Kim, J.C. Choe, M.S. Kim, J. Phys. Chem. A 105 (2001) 5751.

[4] M. Malow, M. Penno, K.M. Weitzel, J. Phys. Chem. A 107 (2003) 10625.

[5] C. Lifshitz, Accounts Chem. Res. 27 (1994) 138.

[6] C. Lifshitz, E. Nadav, M. Peres, T. Peres, J. Laskin, B. Karsenty, M. Shaked, Int. J. Mass Spectr. Ion Processes 133 (1994) L11.

[7] C. Lifshitz, Y. Gotkis, J. Laskin, A. Ioffe, S. Shaik, J. Phys. Chem. 97 (1993) 12291.

[8] T.D. Fridgen, J. Troe, A.A. Viggiano, A.J. Midey, S. Williams, T.B. McMahon, J. Phys. Chem. A 108 (2004) 5600.

[9] P. Ausloos, J. Am. Chem. Soc. 104 (1982) 5259.

[10] W.G. Hwang, J.H. Moon, J.C. Choe, M.S. Kim, J. Phys. Chem. A 102 (1998) 7512.

[11] A. Fernandez, A.A. Viggiano, T.M. Miller, S. Williams, I. Dotan, J.V. Seeley, J. Troe, J. Phys. Chem. A 108 (2004) 9652.

[12] S.T. Oh, J.C. Choe, M.S. Kim, J. Phys. Chem. 100 (1996) 13367.

[13] R.C. Dunbar, J. Am. Chem. Soc. 97 (1975) 1382.

[14] D. Fati, A.J. Lorquet, R. Locht, J.C. Lorquet, B. Leyh, J. Phys. Chem. A 108 (2004) 9777.

[15] J. Grotemeyer, H.-F. Grützmacher, Org. Mass Spectrom. 17 (1982) 353.

[16] MathCAD is a product of MathSoft Engeneering and Education Inc., 2001.

[17] R.G. Gilbert, S.C. Smith, Theory of Unimolecular and Recombination Reactions, Blackwell Science Inc., 1990.

[18] T. Baer, W.L. Hase, Unimolecular Reaction Dynamics: Theory and Experiments, Oxford University Press, New York, 1996.

[19] T. Baer, J.C. Morrow, J.D. Shao, S. Olesik, J. Am. Chem. Soc. 110 (1988) 5633.

[20] G.B. Ellison, G.E. Davico, V.M. Bierbaum, C.H. DePuy, Int. J. Mass Spectrom. Ion Processes 156 (1996) 109.

[21] NIST Chemistry Webbook., 2003.

[22] J. Troe, J. Phys. Chem. 87 (1983) 1800.

[23] R.C. Dunbar, J. Am. Chem. Soc. 95 (1973) 6191.

[24] R.C. Dunbar, J. Phys. Chem. 83 (1979) 2376.

[25] J. Stapleton, R.D. Bowen, D.H. Williams, J. Chem. Soc. Perkin Trans. 2 (9) (1979) 1219.

[26] T. Baer, J. Booze, K.M. Weitzel, Photoelectron photoion coincidence studies of ion dissociation dynamics, in: C.Y. Ng (Ed.), Vacuum Ultraviolet Photoionization and Photodissociation of Molecules and Clusters, World Scientific, Singapore, 1991, pp. 259–296.

[27] C. Praxmarer, A. Hansel, W. Lindinger, Z. Herman, J. Chem. Phys. 109 (1998) 4246.

[28] C. Nicolas, R. Torrents, D. Gerlich, J. Chem. Phys. 118 (2003) 2723.

[29] J. Grotemeyer, H.-F. Grützmacher, in: A. Maccoll (Ed.), Current Topics in Mass Spectrometry and Chemical Kinetics, Heyden, London, 1982, pp. 29–59.